A. Morphologies near the Cloud Point for Anionic Surfactant Solutions

4.1. Introduction

Surfactant molecules when dissolved in water, above its cmc can form various types of aggregates. In general, the micellar structure (shape and size) strongly influences the solution behavior. The size and shape of the aggregates not only depend on the chemical composition, but also get dramatically influenced by solution parameters such as temperature, concentration, *p*H, or ionic strength. Micelles tend to occur in a range of morphologies, including spherical, ellipsoidal, rod shaped, vesicles, lamellar structures, etc under appropriate solution conditions [159-161]. Generally, micellar aggregates are globular in shape at low surfactant concentration and can undergo various such structural transitions, mainly, as a result of an increase in the surfactant concentration, addition of salt as well as increase in the length of the surfactant hydrocarbon chain, changes in pH or any other external stimulus [162-166]. The conditions used for many micellar applications, e.g., biopolymer (DNA [167] or phospholipids [168] processing) may influence the micro -structure. Hence, the knowledge of the factors affecting aggregate formation becomes increasingly important in the physical synthesis of self assemblies. The interfacial water in the immediate vicinity of hydrophobic and hydrophilic surfaces of amphiphile plays a predominant role in various phenomena [36, 169]. It has been well understood that water molecules confined in various micro-heterogeneous nano confinements (like micelles, reverse micelles, liposome, lamellae etc.) behave in a markedly different manner compared to bulk water. The property of the confined water is dependent upon the nature of the surfactant molecule (ionic or nonionic) constituting a self assembly. Various strategies have been employed to controllably attenuate micellar structures [170]. One of the desirable changes to the micellar structures is their growth which is important for various applications in different areas of interest. Different strategies already adopted to bring about the growth in anionic micelles are: addition of oppositely charged surfactant, screening of the electrostatic repulsion by addition hydrotropes (salts or acids) and addition of organic additives (e.g. medium to large chain length alcohols or amines) with and without salt. However, in all above strategies there was an inherent problem of either precipitation or the multi-component system with undefined interactions. Temperature often plays an important role in morphological transitions and other solution behaviour [111,112, 171]. To minimize the above mentioned undesirable effects, a, temperature-induced micro structural transitions could be a better choice. Also, very little is known regarding the morphologies present in ionic surfactant solutions when they approach the CP. Usually the transition from a higher order aggregate to a lower order state takes place on increasing the temperature [113-115]. Among the ionic surfactants, micellar growth behaviour on heating is common only for some cationic surfactants mixed with oppositely charged surfactant/hydrotropes [111,116, 117]. It is generally believed that the size of the ionic micelles reduces when the temperature is raised [172-177]. However, studies regarding the temperature induced micellar growth are so far rare for single anionic surfactant system [98]. In this study the micellar morphological changes near CP could not be well understood due to the appearance of clouding near the ambient temperature.

Based on the above information (also in Chapters 1 and 3) following objectives were set.

To study the ***temperature induced growth*** *with the single ionic surfactant system.*
To study the ***temperature induced growth*** *with the single ionic surfactant system.*
To improve the fundamental understanding of ***morphological transitions taking place near CP with anionic surfactant solution and*** *rationalize the observations through qualitative arguments.*
To study the seldom ***studied salt induced*** *growth in anionic surfactants having quaternary counterion.*
To compare the effect of both temperature and charge of counterion on ***morphological transitions.***

Hence, with the above objectives, various techniques (NMR, DLS and SANS) are used to draw information regarding micro-structural changes in a typical anionic surfactant (scheme, chapter 2) solution on heating. The work performed here covers in detail about: influence of counterion and alkyl headgroup; temperature effect on micellar growth and the possible synergistic effect of salt addition and heating.

4.2. Results and Discussion

4.2.1. DLS measurements

To get an idea regarding the changes in micelle size with an increase in temperature, DLS studies were performed with various surfactant solutions at different temperatures (below and above the CP). DLS data (0.1M TBADS and 0.03 M TBADBS) at different temperatures (Figures 1 and 2), below and above the CP, have shown the development of bigger morphologies (grown micelles) at the cost of smaller ones (in addition to smaller ones) even below CP. It was observed that two populations of different sizes are present near the CP suggesting two types of micelle morphologies in the solution when it is about to reach CP.

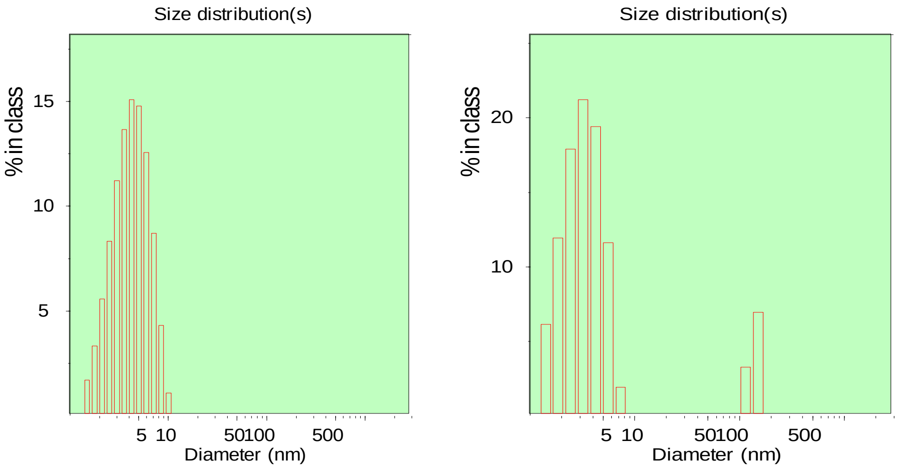

(a) T=25°C (b) T= 28°C

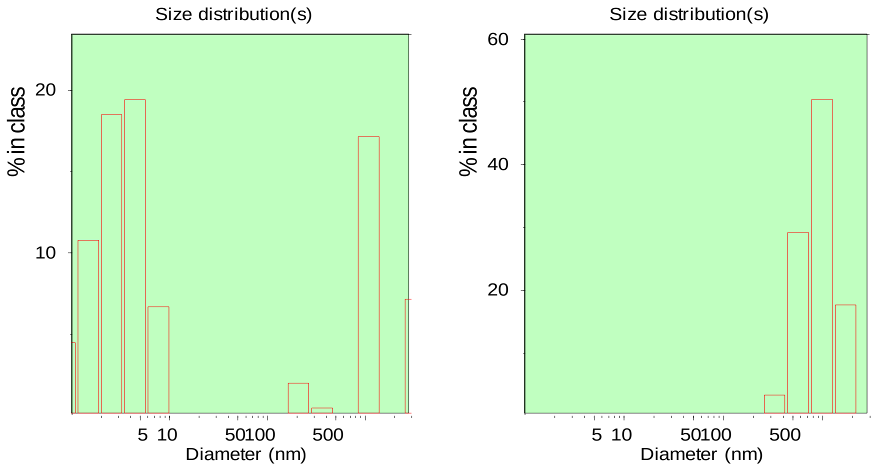

(c) T=32°C (d) T=35°C

Figure 1: DLS data at different temperatures below (a and b), near (c) and above CP (d) of 0.1 M TBADS (CP = 32.1 °C).

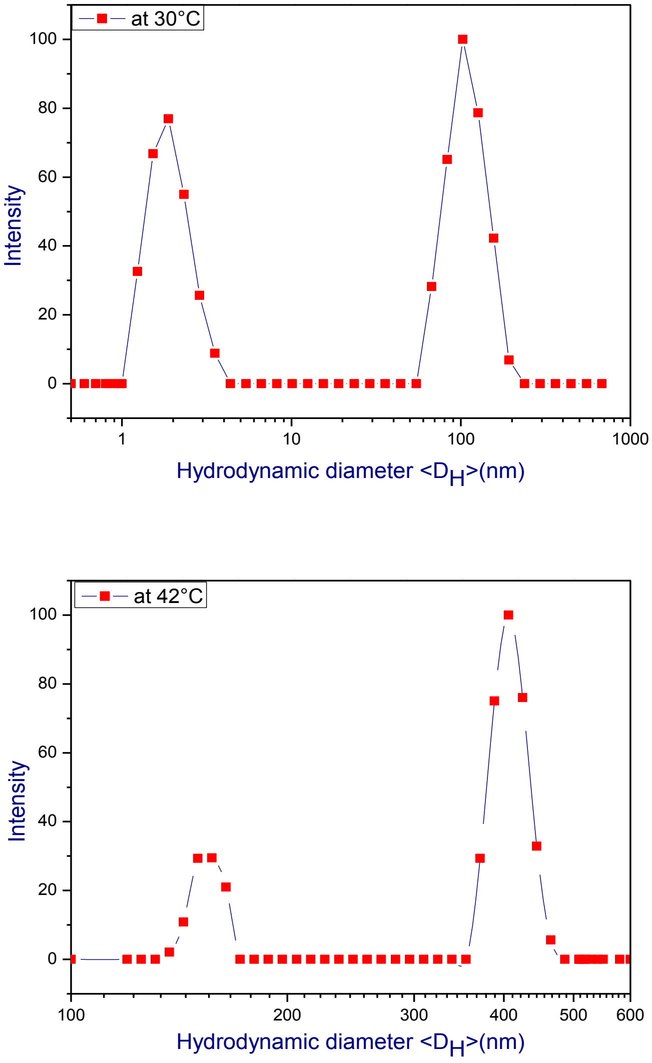

Figure 2: DLS data of 0.03 M TBADBS at (a) 30 °C and (b) near CP (= 42.5 °C)

From the lognomal distribution it was intimated that D_H increases considerably near the CP (Figure 3a). Linking of grown micelle may start, at a particular temperature which then leads to the formation of bigger aggregates responsible for clouding phenomenon. After CP, two phases slowly separate and one of the two phases now spans the whole scattering volume. This is in consonance with the decrease in size after CP. As the micelles are growing with increasing temperature, the ratio of the fraction of bigger micelles to that of smaller ones increases with the increase of temperature, leading to the increase in polydispersity (Figure 3b). However, after certain temperature, the micelles are grown rapidly (with a decrease in number density) and hence responsible for lowering in the polydipersity. This is also an indication of the dominance of one of the populations. Interestingly, the polydispersity of the system reaches to minimum, as the phase separation starts. It can be said that only one of the two phases now spans the whole scattering volume tending the system towards the mono-dispersed phase.

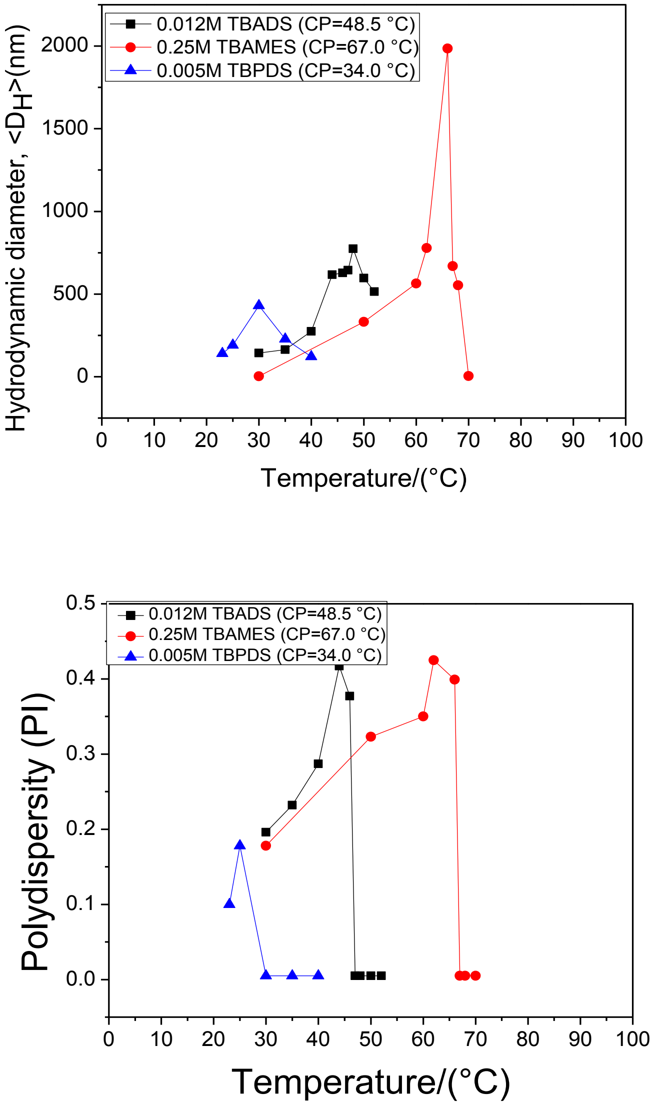

(A)

(b)

Figure 3: Temperature effect on a) hydrodynamic diameter <D_H> and b) polydispersity (PI) of different surfactants solutions

4.2.2. SANS measurements

SANS measurements provide useful information pertaining to the micelle growth and fractional charge for different anionic surfactant solutions in a non-invasive manner. SANS spectra of 0.0124M TBADS as a function of temperature before and after the CP is shown in Figure 4. On increasing the temperature, $d\Sigma/d\Omega$ decreases remarkably in low Q region. This is a typical behaviour observed earlier [98]. The purpose of the present temperature effect study was to have enough temperature range below and above the CP. Therefore, a lower concentration (0.0124M TBADS; CP=46.0°C) has been chosen. No significant change was observed in fitted micellar parameters when the solution temperature reaches near the CP (Table 1). Once the CP crosses, magnitude of scattering intensity curve starts decreasing in the low Q region. This means the number density of individual micelles on heating decrease as the grown micelles fuses via butyl chains of dehydrated TBA^+ and form bigger aggregates. Size of the bigger aggregates is expected to be out of range of the present SANS spectrometer. This actually is seen from the decrease in micellar fraction of individual micelles (which now spans the whole scattering volume) with the increase in temperature after CP. From earlier studies [100] it is seen that only 40% of the TBA^+ counterions are adsorbed at the micelle surface due to their bulky nature. Also, it has been reported that only two butyl chains (due to the geometric restrictions) can intercalate into the micellar core and about 75% volume of these tail reside in the micellar core. The intercalation of dehydrated TBA^+ (at higher temperature near CP), between the anionic head groups screens the charge, reduces electrostatic repulsion. Hence, the overall charge on micelle surface decreases (Table 1), which is responsible for their pseudo nonionic character.

The scattering from the individual micelles exist at and even beyond CP suggesting that only a fraction of total micelles (grown) fuses via dehydrated counterions, forming bigger aggregates responsible for clouding as also hinted by DLS data (*vide supra*). On further increasing the temperature, more micelles grow and participate in forming bigger aggregates responsible for clouding resulting in further decrease of individual micelle fraction. Thus, the study intimates that conversion of individual micelles to giant aggregate may be the reason of clouding specifically in ionic surfactant solution (e.g TBADS). The process of clouding as observed seems to be more gradual than that in nonionic surfactant solutions. This may be due to the presence of charged micelles in the former case.

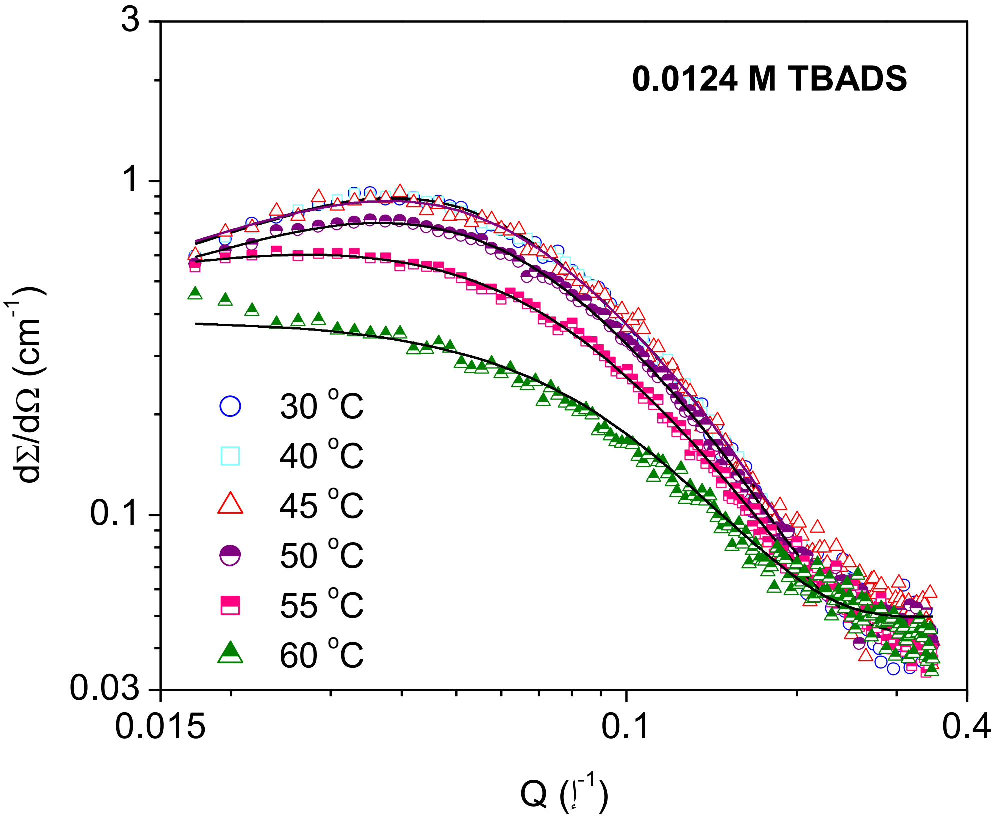

Figure 4: SANS spectra of 0.0124 M TBADS at varying temperatures below and above CP.

Table 1: Fitted micellar parameters of 0.0124 M TBADS at varying temperatures using model for prolate ellipsoidal.

Temperature (^{o}C)	Semiminor axis b=c (Å)	Semimajor axis a (Å)	Aggregation number N	Fractional charge α	Micellar fraction (%)
30	14.6	47.8	73	0.11	100
40	14.5	50.0	75	0.11	100
45	14.4	51.3	75	0.11	100
50	14.3	46.5	67	0.10	87
55	13.8	41.9	55	0.06	70
60	13.8	36.1	46	0.02	40

SANS data with 0.03M TBADBS (CP =39.0 °C) (Figure 5) show a variation in interaction peak and magnitude of intensity with increase in temperature. From the analyzed data (Table 2) a significant micellar growth has been seen when compared to TBADS for the same concentration (0.03M) [178]. This may be due to the structural difference between these two surfactants (an extra benzene ring and a less hydrated alkyl sulfonate group). These structural differences are responsible for increased interaction with TBA^+ with a concomitant increased micellar growth in case of TBADBS on heating. In case of TBADBS the results show that the semi-major axis increases from 200.0 to 257.0Å as the temperature approaches near CP. Beyond the CP, aggregates are large enough and seems responsible for a drastic decrease in the cross section. This actually is seen from the decrease in micellar fraction of individual micelles (which then span the whole scattering volume) with the increase in temperature after CP. Here too, the scattering from the individual micelles exist at and even beyond CP. The temperature increase causes loss of hydrogen bonding [179] and the counterion condensation that drives the growth of micelles.

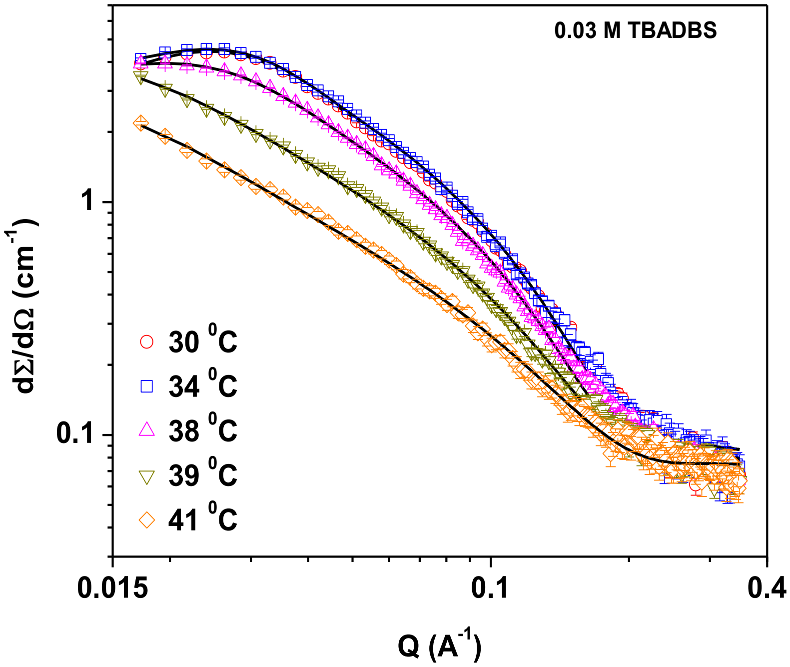

Figure 5: SANS spectra of 0.03M TBADBS at different temperatures below and above CP.

Table 2: Fitted micellar parameters of 0.03 M TBADBS at varying temperatures using model for prolate ellipsoidal.

Temperature (°C)	Semiminor axis b=c (Å)	Semimajor axis a (Å)	Aggregation number N	Fractional charge α
30	18.5	200.0	366	0.05
34	18.3	200.0	366	0.05
38	18.5	257.0	471	0.03
39	16.1	-	-	-
41	15.5	-	-	-
43	-	-	-	-

To get further insight, the temperature effect is also studied with TBAMES. The extra ester group in TBAMES (scheme, chapter 2) may form H-bond with water molecule owing to dipole-dipole interaction. This results in increased hydration responsible for higher CP. It gives clouding at higher temperature and at comparatively higher concentration than TBADS and TBADBS which may provide enough temperature range to study the effect. SANS spectra of 0.25M TBAMES (CP=65°C) at various temperatures are shown in Figure 6. There is an increase and then decrease in the scattering cross-section in the low Q region on continuous increase in temperature. For conventional ionic micelles the scattering cross-section usually decreases with temperature due to modifications in the structure and interaction of the micelle. An increase in scattering cross-section on heating for non-ionic micellar solutions has been reported. From the figure it is seen that TBAMES solution behaviour overlaps with both conventional ionic and non-ionic micellar solutions on heating. Table 3 contains fitted micellar parameters which show that length of semi-major axis (a) increases with temperature from 28.1 to 89.2 Å confirming the micelle growth on heating. The behaviour can be understood in the light of the fact that dehydrated TBA^+ counterion associate with ionic micelle to form grown micelles at higher temperature (near CP) and decrease the electrostatic interactions. This is clearly reflected by the lower α values. Here, along with the micelle growth, the onset of attractive interaction is also confirmed from the low Q upturn (inset figure) with the increase in temperature. Thus a general trend of micelle growth with increase in temperature has been observed with synthesized quaternary surfactants.

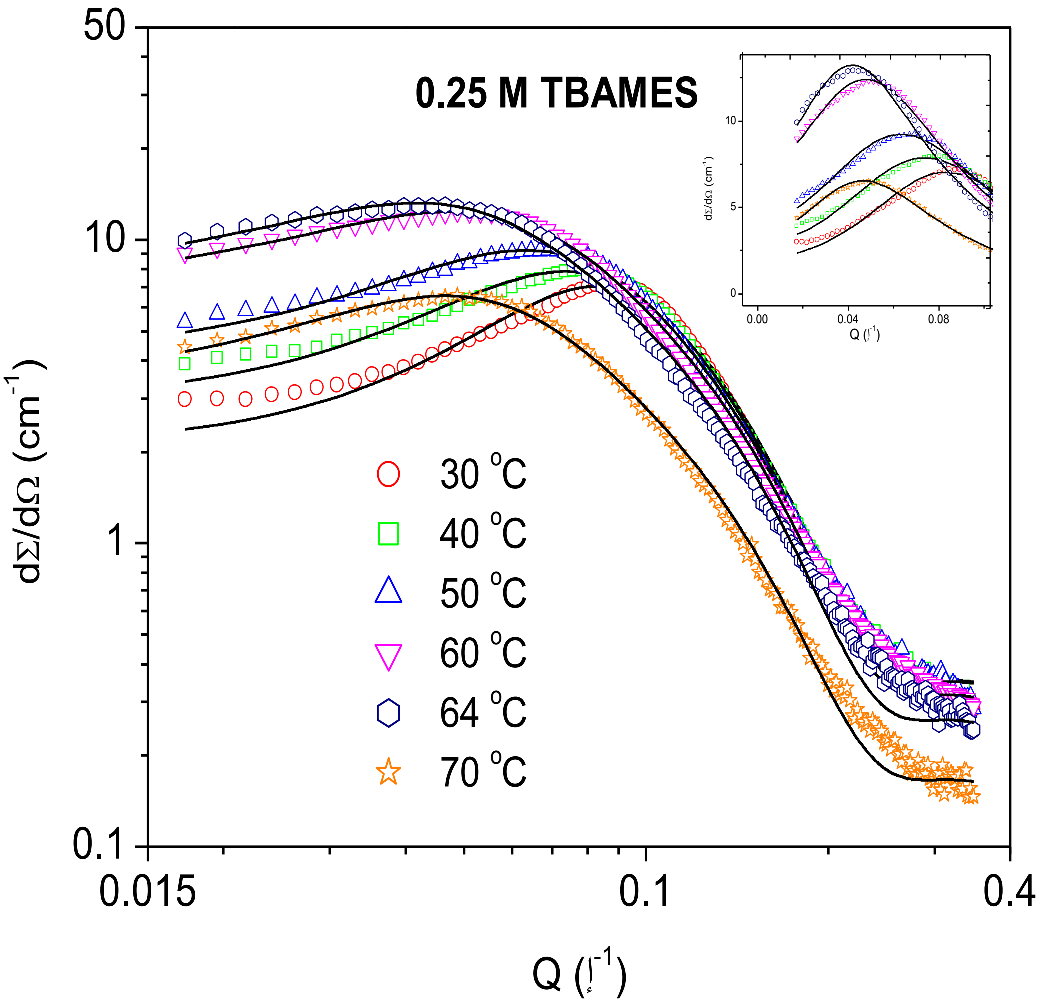

Figure 6: SANS spectra of 0.25M TBAMES at different temperatures below and above CP

Table 3: Fitted micellar parameters of 0.25 M TBAMES at varying temperatures.

Temperature (^oC)	Semiminor axis b=c (Å)	Semimajor axis a (Å)	Aggregation Number N	Fractional charge α	Micellar fraction (%)
30	16.0	28.1	50	0.06	100
40	16.0	30.5	54	0.06	100
50	16.0	35.6	62	0.05	100
60	16.0	50.7	87	0.04	100
64	16.0	89.2	151	0.03	100
70	16.0	81.8	139	0.01	48

Figure 7 shows the concentration effect on the SANS data of TBAMES. Scattering patterns are similar to the spectra observed earlier for anionic micelles. The spectra shifted to higher Q values which is obvious on increasing concentration of the surfactant (due to increase in number of micelles). This indicates that the nature of the micelles at 30°C is similar to the conventional ionic surfactant. The analyzed data are given in Table 4, which show that the aggregation number decreases at higher [TBAMES]. This behavior is different than the conventional ionic surfactant like SDS. The key lies in the structure of TBAMES molecule which contains an ester group near the head group region. When concentration increases, more hydrated water will be present in the micelle with a simultaneous decrease in the aggregation number as hydration of the monomer works against association. This may be the reason of the decrease in aggregation number (N) and increase in fractional charge (α).

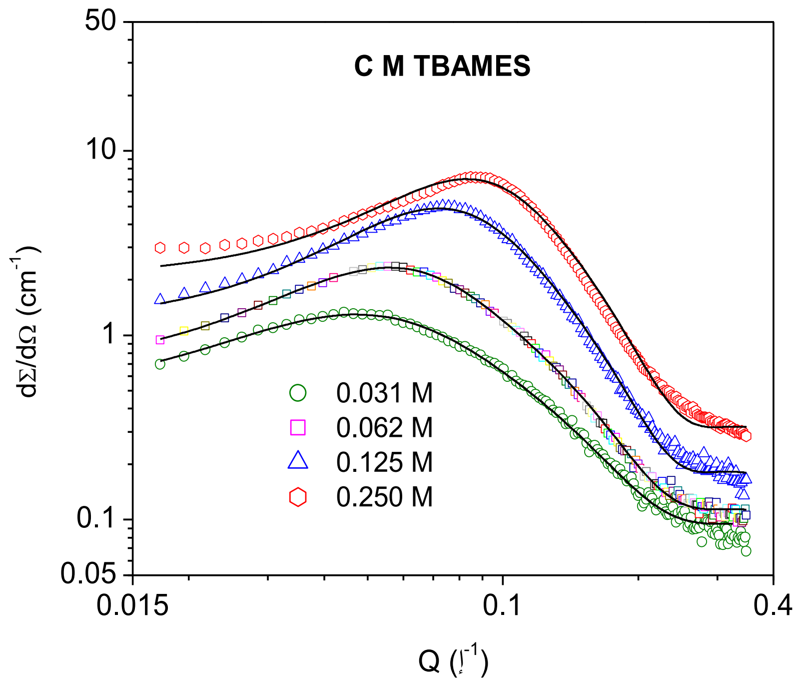

Figure 7: SANS spectra of TBAMES at different concentrations at 30 ^{o}C.

Table 4: Micellar parameters of TBAMES with varying concentrations.

Concentration (M)	Semiminor axis b=c (Å)	Semimajor axis a (Å)	Aggregation number N	Fractional charge α
0.031	15.5	40.2	62	0.12
0.062	15.5	40.9	66	0.12
0.125	16.0	32.6	57	0.14
0.250	16.0	28.1	50	0.17

However, in earlier studies [80,113] micellar disintegration is reported for charged micelles on heating. SANS spectra for SDS, being a typical conventional anionic surfactant (not showing clouding) is shown in Figure 8. From the fitted micellar parameters of 0.03M SDS solution (Table 5) it is seen that ellipsoidal micelle disintegrate (decrease in semi major axis (23Å to 19.7Å) on increasing the temperature from 30°C to 60°C).

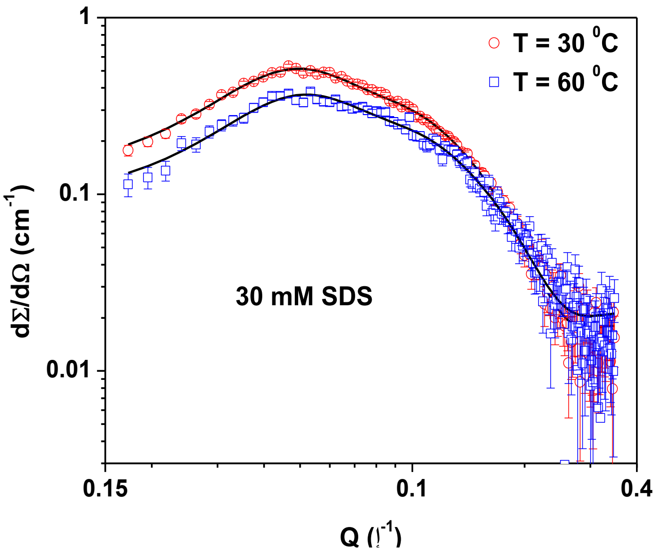

Figure 8: SANS data of 0.03M SDS micelles at two temperatures.

Table 5: Fitted parameters for 0.03M SDS micelles at different temperatures using model for prolate ellipsoidal.

Temperature (°C)	Semi-major axis a (Å)	Semi-minor axis b=c (Å)	Fractional Charge α	Aggregation Number N
30	23.0	15	0.46	62
60	19.7	15	0.49	53

This study is extended to TX-100, a well known conventional non ionic surfactant showing clouding on heating. Neither any micelle growth nor the micellar shape change is reflected in the SANS analysis (Table 6). However, the low Q upturn with increasing temperature due to the attractive interaction is the predominating factor responsible for clouding. (Figure 9 and Table 6).

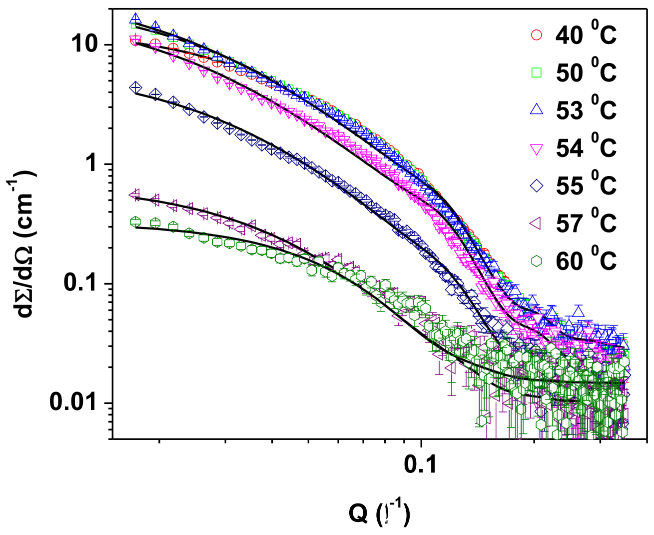

Figure 9: SANS data of 2% TX100 (CP=54°C) system at different temperatures using Oblate ellipsoidal model.

Table 6: Fitted parameters for TX100 micelles at different temperatures using model for oblate ellipsoidal model with structure factor calculated for sticky hard sphere.

Temperature (^{o}C)	Semi-major axis b=c (Å)	Semi-minor axis a (Å)	Volume fraction ϕ	Micellar Fraction %	Stickiness (1/ τ)
40	46.8	17.2	0.13	100	5.55
50	47.2	17.3	0.13	100	7.1
53	46.7	17.2	0.13	100	7.7
54	46.1	17.8	0.13	77	7.7
55	46.8	17.0	0.1	30	7.7
57	46.7	17.1	0.05	15	7.7
60	46.7	17.2	0.01	7	7.7

4.2.3. NMR measurements

The ^{1}H NMR spectroscopy has been found one of the convenient methods for the monitoring of changes in aggregate morphology by knowing the value of δ for different protons present in the typical surfactant. The spectra of TBADS in D_2O at different temperatures are collected. The observed δ values are comparable with the reported work [101] NMR data show the shifting of spectra as a whole to higher δ (ppm) scale (downfield) together with broadening of a few peaks as the temperature increases (Figure 10). This suggests that the dehydration of TBA^+ (–N-CH_2 peak, N1) and micellar head group (-O-CH_2 peak, S1) region takes place together with the micellar growth [180, 181].

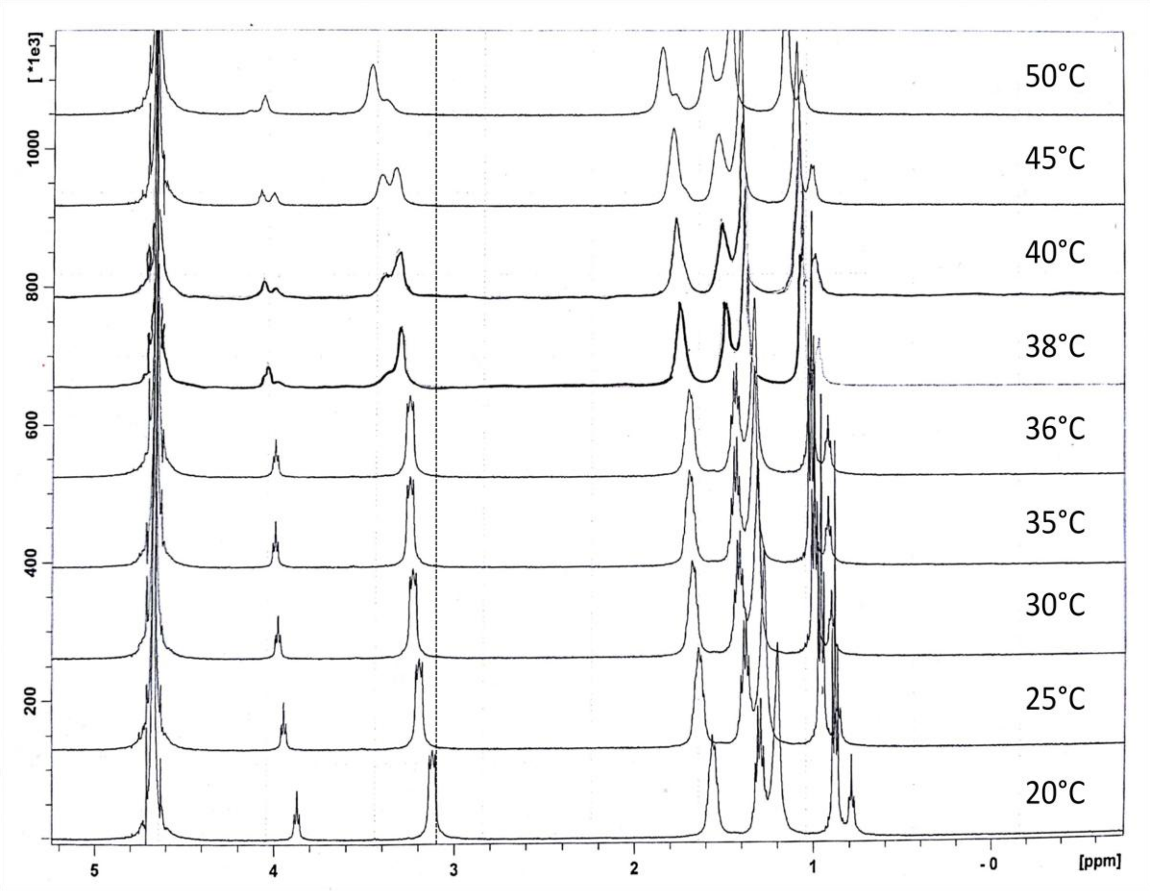

Figure: 10 ^{1}H NMR spectra of 0.03M TBADS solution at different temperatures

The decrease in electron density around proton is supported by deshielding with the increase in temperature. The higher δ values also corroborate the increase in attractive forces resulting in clustering of micelles responsible for giant aggregates. The N1 proton peak of TBA^+ at 3.2 and S1 peak of DS^- at 3.95 show the gradual splitting into two separate peaks due to the alteration of the chemical environment around above two protons (Figure 11). The NMR data depict that the above two protons are distributed between two different morphologies (individual micelles and giant aggregates).

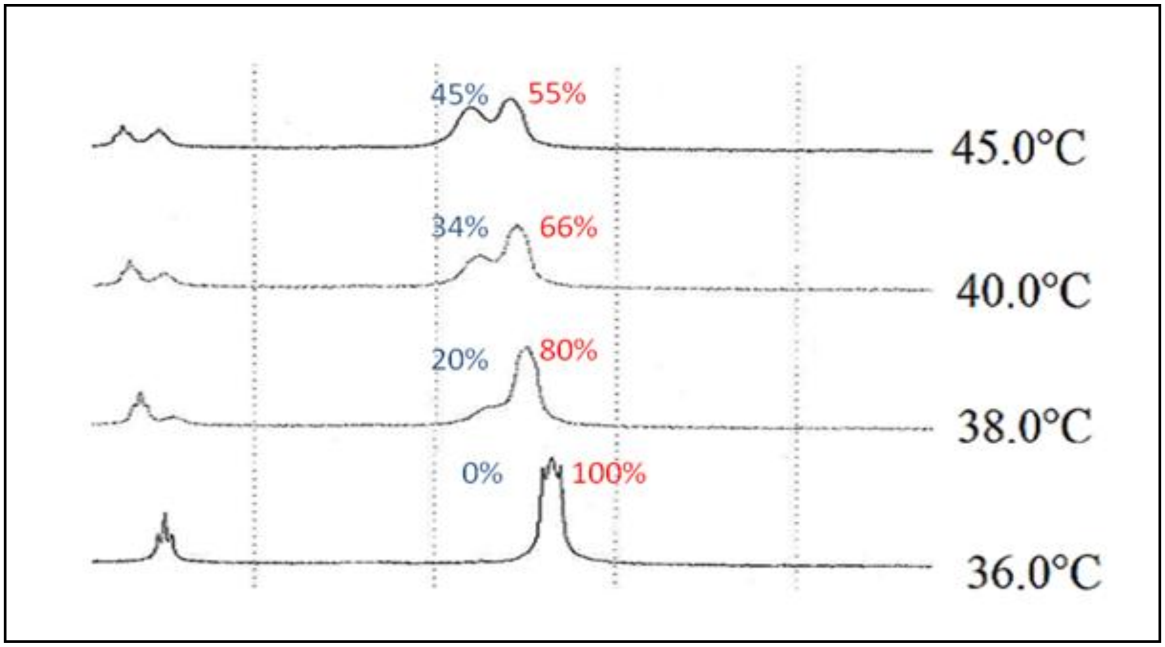

Figure 11: ^{1}H NMR spectra for –O-CH_2 and –N-CH_2 protons in 0.03M TBADS solution at different temperatures showing the % of two morphologies (individual micelle, % and giant aggregate, %)

Similar results are obtained with 0.0124M TBADS with the only difference in the % conversion (Figure 12). Below CP, 100% individual micelles are present. It can be observed that individual micellar volume fraction decreases as the temperature passes the CP whereas the % of the giant aggregates increases at the cost of individual micelles. The rate of conversion of individual micelles to giant aggregates, on heating, seems dependent upon the initial concentration of TBADS taken. For 0.03M TBADS (CP=36.5°C), at 38°C, 20% micellar fraction converted into the giant aggregates. However, for 0.0124M

TBADS (CP=46.0 °C), at 48°C, the fraction was ~ 15%. At higher temperature, irrespective of the concentration and CP, the dehydrating factor dominates and the conversion rate increases as more and more TBA$^+$ are available in the bulk to facilitate linking, resulting in the giant aggregates.

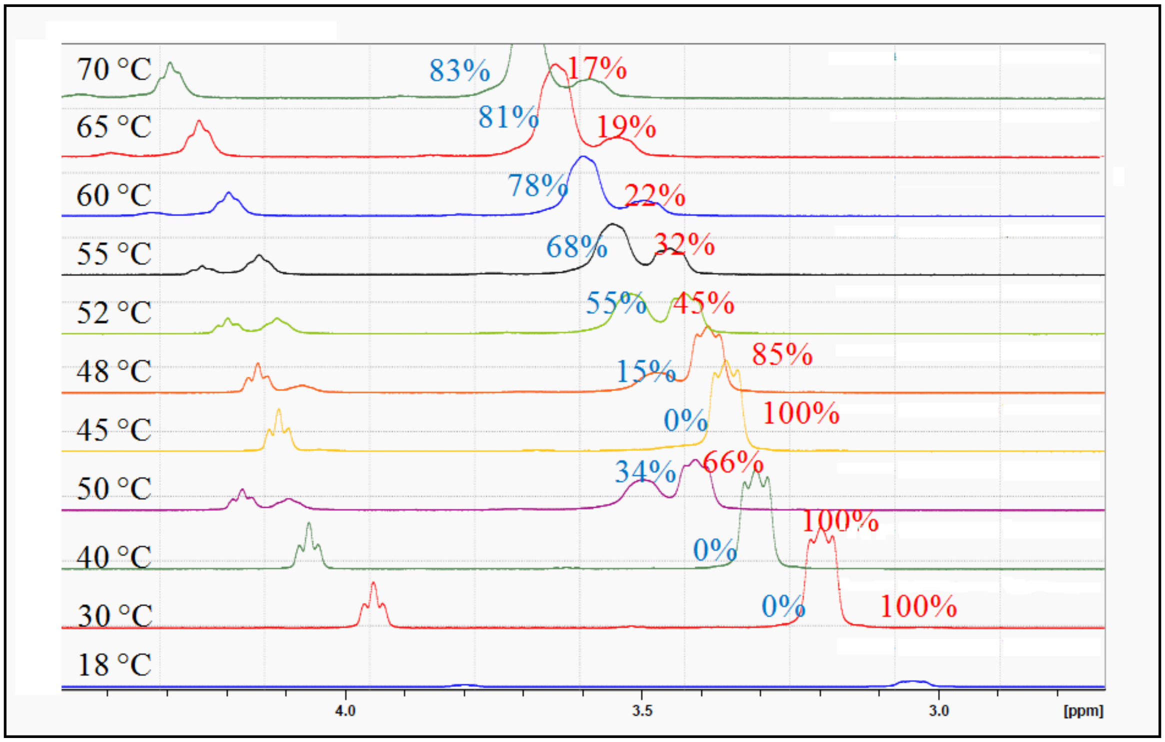

Figure 12: NMR Spectra for –O-CH_2 and –N-CH_2 protons in 12.4mM TBADS solution at different temperatures showing two morphologies as it passes CP.

NMR data for TBADBS with increasing temperature is also collected. The -NCH_2 proton in 0.015M TBADBS; (Figure 13) also splits into two peaks as observed in TBADS and can be understood as discussed above. However, peak splitting effect for 0.03M TBADBS solution (Figure 14) has not been observed on heating. But a gradual broadening of above peak (N1) again indicates about the growth in micellar morphology.

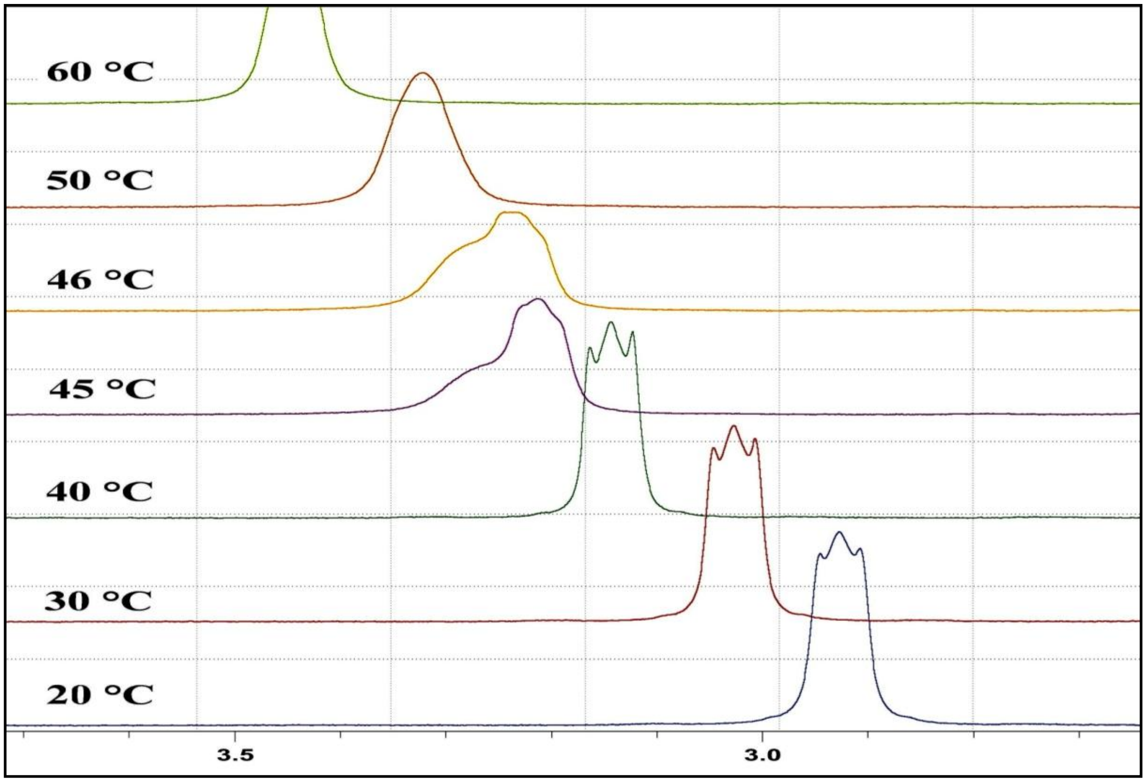

Figure 13: ^1H NMR spectra for −N−CH_2 (N1) protons in 0.015M TBADBS solution at different temperatures (below and above CP) showing the broadening and splitting of the peak into two different morphologies.

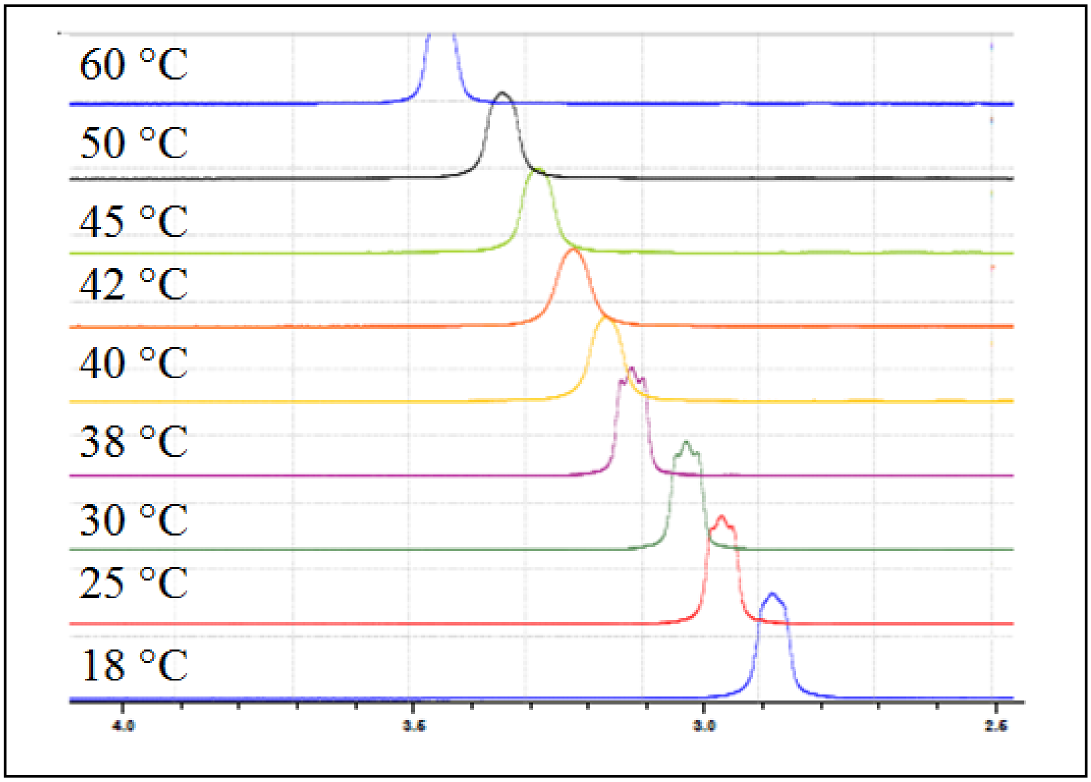

Figure 14: ^{1}H NMR spectra for −N−CH_2 protons in 0.03M TBADBS solution at different temperatures (below and above CP) showing the broadening and splitting of the peak

The spectra of TBAMES in D_2O at different temperatures are shown in Figure 15. The spectra can also be interpreted in the light of above facts discussed in case of TBADS/TBADBS. Thus, the decrease in degree of hydration, increase in attractive forces (between the counterions and the micellar head group) and formation of two morphologies (individual micelles and giant aggregates) can be explained as a general trend, for quaternary surfactants. Though, NMR is not directly sensitive to the morphological transitions, they can be assessed from the variation in δ values and broadening of different protons. However, the technique can be utilized to draw informations regarding morphology of the micelle when used in combination of other technique(s).

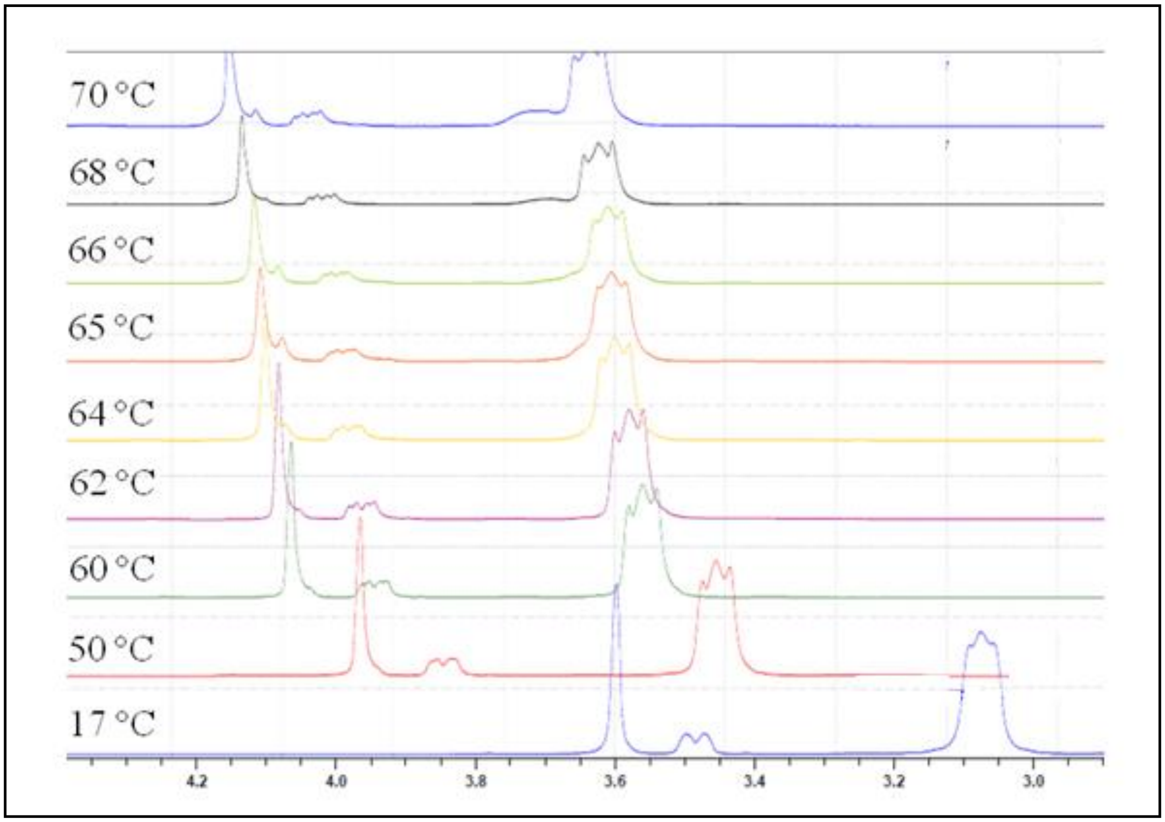

Figure 15: NMR Spectra for –O-CH$_2$ and –N-CH$_2$ protons in 0.25M TBAMES solution at different temperatures showing two morphologies as it passes CP.

The ^{1}H NMR spectra of 0.05M TBPDS (CP=27°C) at variable temperatures show the similar δ changes and broadening as observed above for –P-CH$_2$ (Figure 16a). Due to the dehydration of counterion and the surfactant head group, the counterion condensation takes place which may be responsible for growth of the micelles. This may find support from the fact that *P* value can increase due to lowering in the value of a_0. The increase in *P* is always reported for the formation of higher order aggregates [116]

To show the counterion effect without the interference of other neighboring protons, ^{31}P decoupled NMR spectra, at different temperatures, were also acquired with 0.05M TBPDS (Figure 16b). The similar broadening and splitting of the –P-CH$_2$ peak corroborates the ^{1}H NMR results.

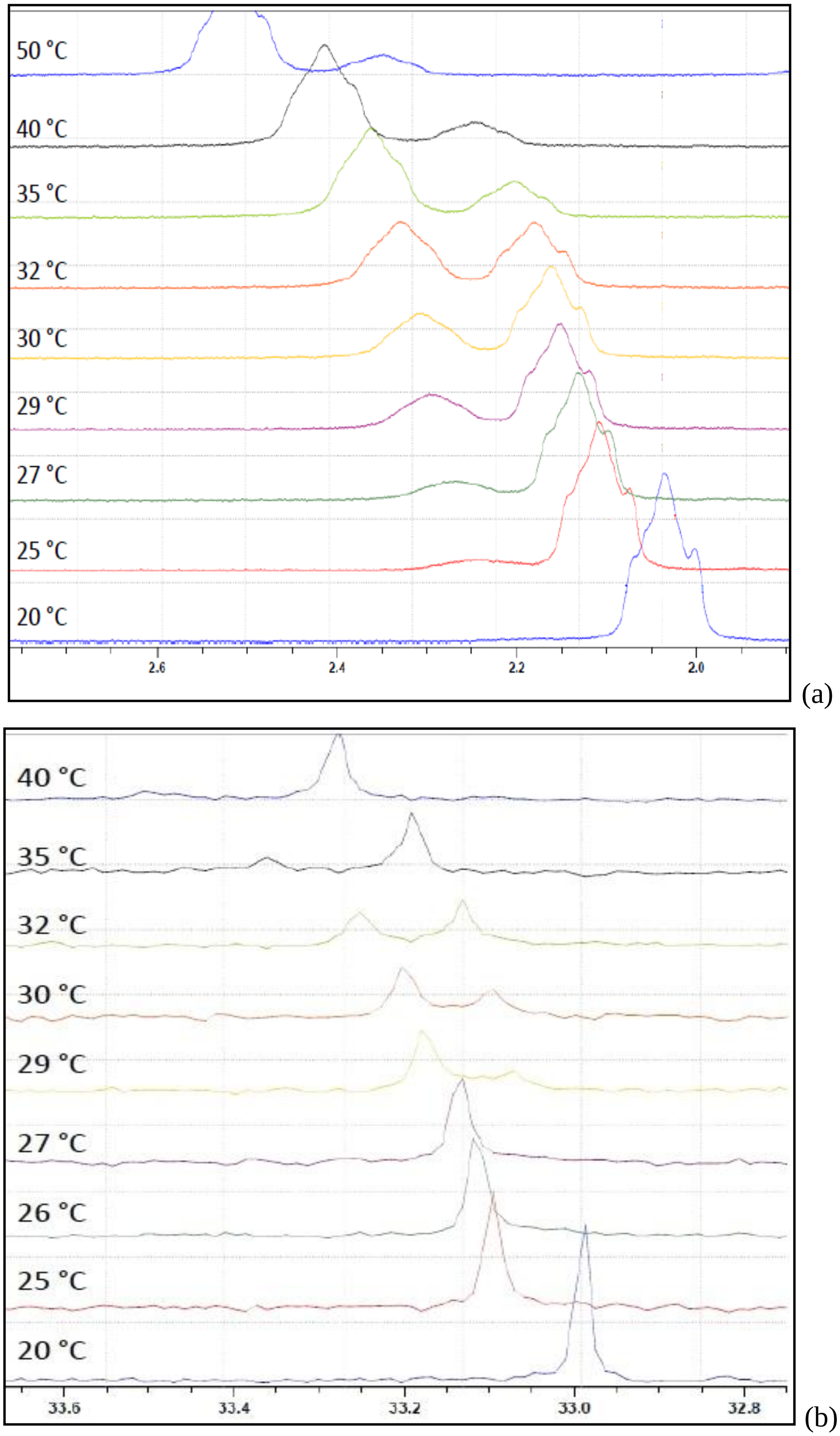

Figure 16: NMR spectra a) ^{1}H and b) ^{31}P for 0.05M TBPDS at different temperatures below, at and after CP.

This study was extended to 2% TX-100 (CP=52 °C), a well known conventional nonionic surfactant, showing clouding on heating wherein no such broadening and splitting of peaks is seen on heating till CP (Figure 17). This may be due to the presence of more hydrophilic units present in the chain which on heating may only dehydrate and decrease the polar character of the poly(ethylene glycol) headgroup, giving rise to the attractive interactions responsible for clouding[105]. In fact the decrease in electron density around proton supported by higher δ values with the increase in temperature corroborates the increase in attractive forces resulting in clustering of micelles responsible for CP.

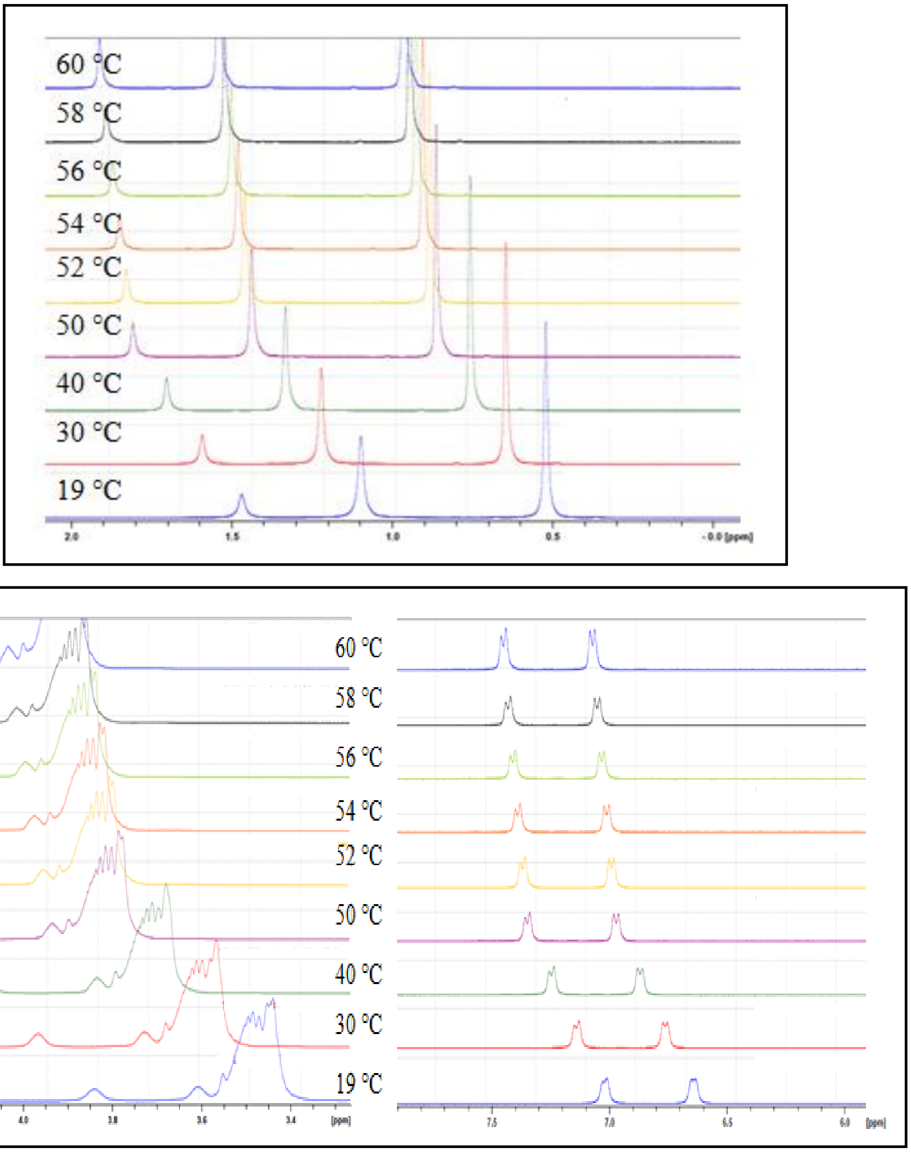

Figure 17: NMR spectra a) ^{1}H for TX-100 at different temperatures below, at and after CP

B. Morphologies near the cloud point for Anionic surfactant solutions in presence of salts.

4.2.4. DLS measurements

Representative DLS data for 0.03M TBADBS in absence/presence of 0.5 mM salt (NaCl, $Mg(NO_3)_2$ or $Al(NO_3)_3$), at 30 °C and near the CP, are shown in Figure 18. DLS data (near CP) show an increase in D_H when compared to data at 30 °C. A significant micelle growth, in presence of Mg^{+2}/Al^{+3}, has been observed. At 30 °C the two distributions were ~50-50 % say for e.g., in case of Mg^{+2}. Whereas, near CP, this ratio has changed (increased % of giant aggregates), and overall D_H has also shifted to higher side indicating the growth of all the micelles (Table 7). This indicates the significant interaction of Mg^{+2}/Al^{+3} with the micellar surface. This may be due to the fact that a multivalent counterion can bind with more than one headgroups causing a faster decrease in a_0. In accordance with the theory by Israelachvili et al., [29] this can facilitate the formation of higher order aggregates. Thus, temperature and valence of the counter ion show a synergistic effect in micellar growth.

Table: 7 DLS data showing the % (~) of two morphologies (individual micelle, and giant aggregates) at 30 °C and near their respective CPs.

	0.03M TBADBS+0.0/0.5mM salt							
Temperature	No salt		Al^{+3}		Mg^{+2}		Na^{+}	
	%	%	%	%	%	%	%	%
30 °C	40	60	70	30	50	50	70	30
Near CP (°C)	40*	60*	20	80	10	90	50	50

* Toward higher D_H

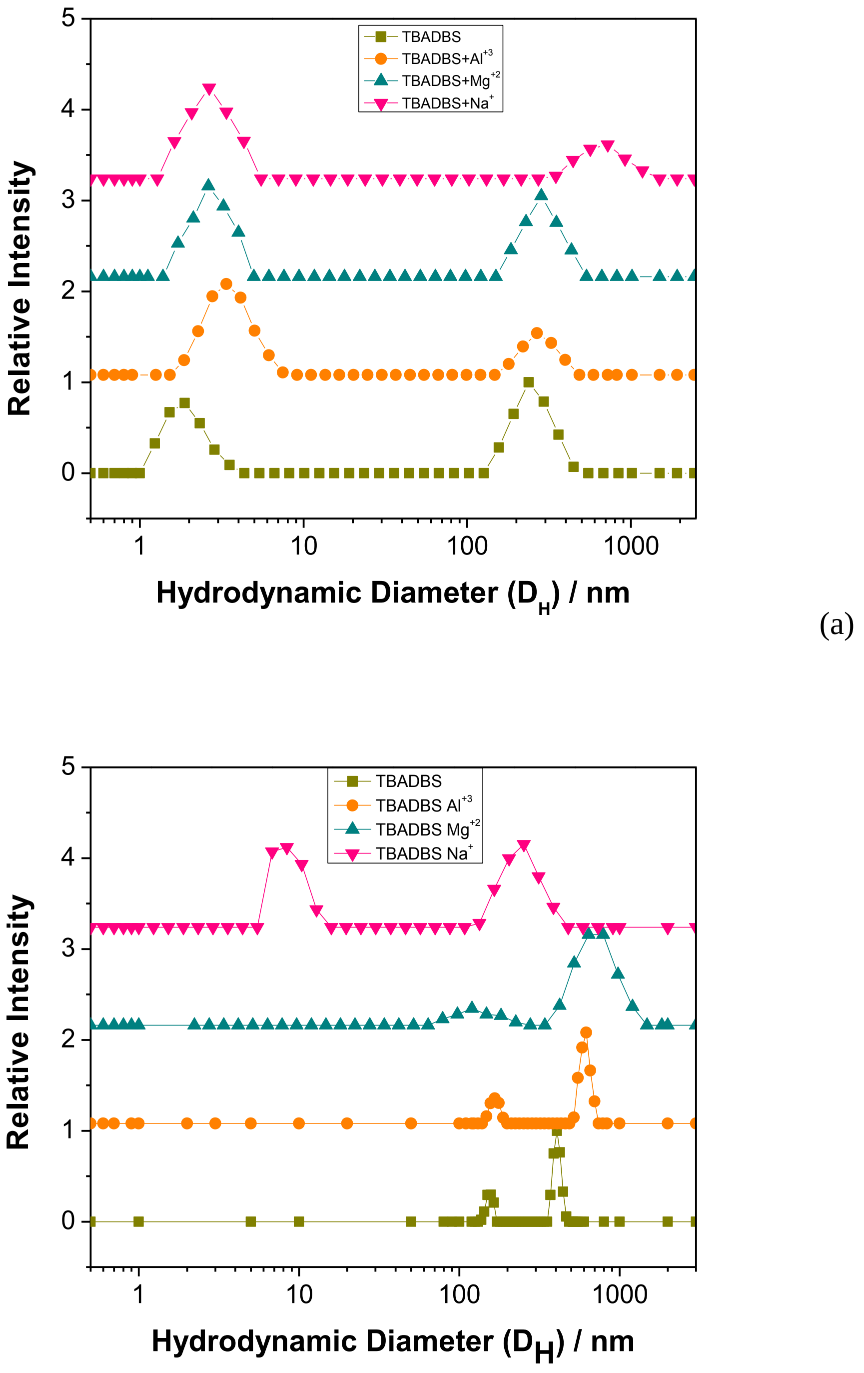

Figure 18: DLS data for 0.03M TBADBS in absence and in presence of $0.5*10^{-3}$M $Al(NO_3)_3$, $0.5*10^{-3}$ M $Mg(NO_3)_2$ and $0.5*10^{-3}$M NaCl at a) 30 °C and b) near CP.

4.2.5. SANS measurements

To further confirm the synergistic effect of temperature and salt in micellar growth, SANS data of 0.03M TBADS with different salts at 30°C and at just below the CP are acquired. The scattering cross section near the CP, decreases, except in case of NaCl (since the [NaCl] is in the range, of increasing CP), indicating the variation in micelle number or size on heating (Figure 19). The fitted micellar parameters, with and without addition of inorganic salts, are compiled in Table 8. For pure 0.03M TBADS, micelles are ellipsoidal in nature. Addition of 0.05M NaCl to 0.03M TBADS solution causes decrease in micelle size at 30°C. However, on addition of 0.05M $Mg(NO_3)_2$ the micelle size increases significantly even at 30°C. The scattering data (Figure 19b) in the low Q region follow a linear pattern on log-log scale having slope of -1 which is the characteristic of rod-like micelles. The behaviour of two salts is quite different and depends on the nature/charge of the counter ion. In the case of an inorganic salt, one can expect an exchange of bound TBA^+ by the inorganic counter ion. During this exchange Na^+ may carry more water towards micellar surface in comparison to the case when only TBA^+ was present. This additional hydration may cause decrease in hydrophobic interactions and hence in Nagg. Irrespective of the higher hydrated radii [182], the charge on the added counter ion plays an important role. The effectiveness of Mg^{+2} counter ion may be due to its additional positive charge which can influence both exchange (with TBA^+) and electrostatic attraction with the head group. This indeed is observed from SANS data (Table 8). To get further insight, we have also seen the effect of addition of $Al(NO_3)_3$. Here, a small concentration (0.002M) was enough to get CP at 35.5 °C. This hampered our study at 0.05M $Al(NO_3)_3$ as performed with other salts (NaCl or $Mg(NO_3)_2$. The SANS data with 0.002M $Al(NO_3)_3$ (Table 8) show that micelles are growing on heating and almost half of the individual micellar fraction converted into giant aggregates. This indicates that trivalent counter ion (Al^{+3}), even at low concentration (0.002M), is more effective in producing larger aggregates (not seen by SANS) than monovalent Na^+ (at 0.05M). This may be due to the fact that Al^{+3} may exchange TBA^+ more effectively which can then be used to link more micelles altogether in the process of giant aggregate formation. The data explicitly show the importance of magnitude of charge on the counter ion in micellar association process. Talmon et al [57] discussed the phenomenon of similar micellar growth, where both the mean micelle contour length and average micelle hydrodynamic diameter increases with temperature for an aqueous non ionic surfactant. The large rod-shaped micelles formed in these systems coalesce to form still higher order aggregates with bigger hydrodynamic diameter [45] which causes a phase separation.

To see the effect of alky head group, the study was extended to 0.03M TBADBS with different salts. The SANS data of 0.03M TBADBS with different salts at 30°C and just below CP are shown in Figure 20. The scattering cross section decreases in each case near the CP indicating the variation of micelle number density or size on heating. The fitted micellar parameters for 0.03M TBADBS with various inorganic salts at 30°C and near the CP (of respective samples) are compiled in Table 9. Due to lower CP values for each sample, salt concentrations taken are relatively lower. The general effects are similar as observed with TBADS (Table 8). There is a strong scattering (Figure 20) observed from the clusters in the low Q region for 0.03M TBADBS+$Mg(NO_3)_2$/$Al(NO_3)_3$ samples, which is an indication of large sizes of the clusters at CP. The measured data are the Porod scattering from the clusters. This Porod scattering may arise due to the large clouds formed by the linking of individual micelles. There is, however, no peak observed corresponding to any inter micellar correlations inside the aggregates.

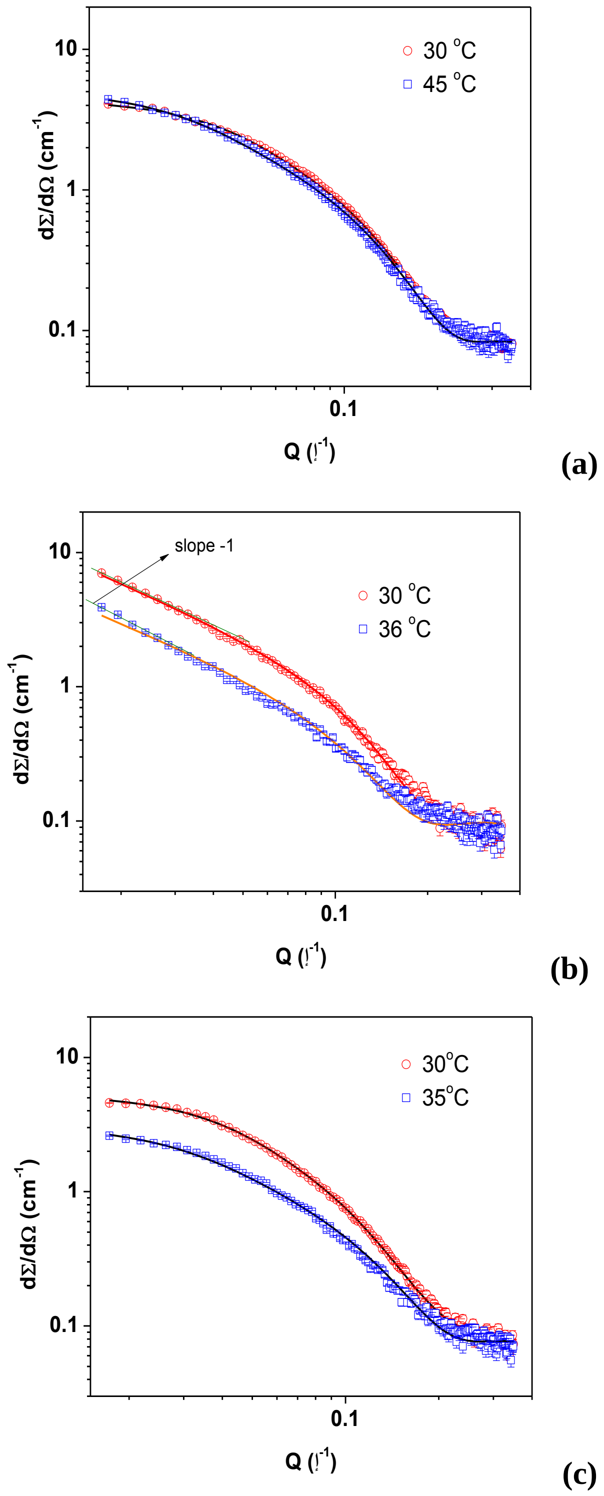

Figure 19: SANS spectra of 0.03M TBADS with a) 0.05M NaCl, b) 0.05M $Mg(NO_3)_2$ and c) 0.002M $Al(NO_3)_3$ at 30(°C) and near CP

Table 8: Micellar parameters of 0.03 M TBADS with and without inorganic salts at 30(°C) and near CP.

0.03M TBADS+Salt	Temperature (°C)	Semiminor axis b=c (Å)	Semimajor axis a (Å)	Porod law (α)	Remarks	Aggregation number Nagg	Micellar fraction (%)
No salt	30	16.0	88.4	-	-	155	100
	-	-	-	-	-	-	-
0.05M NaCl	30	16.0	67.2	-	-	116	100
	45	16.0	88.5	-	-	153	90
0.05M $Mg(NO_3)_2$	30	15.7	-	-	Slope is nearly -1.	-	-
	36	16.8	-	-	-	-	-
0.002M $Al(NO_3)_3$	30	16.0	70.3	-	-	121	100
	35	16.0	85.1	-	-	147	51

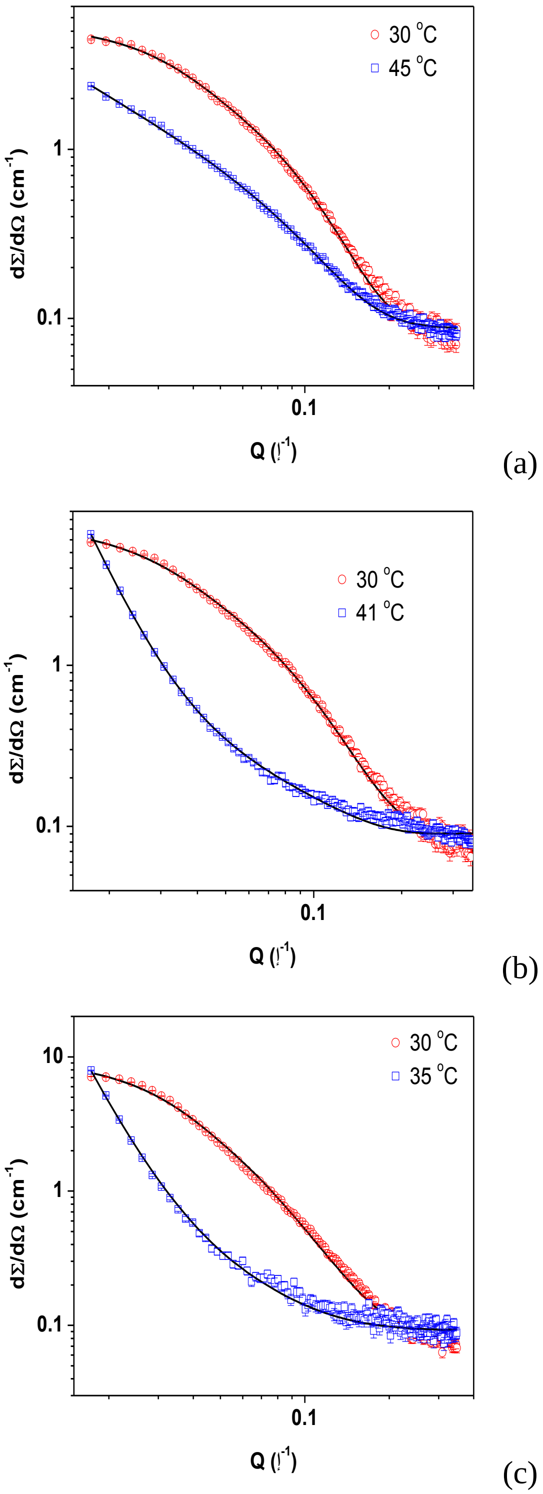

Figure 20: SANS spectra of 0.03M TBADBS with a) 0.005M NaCl, b) 0.001M $Mg(NO_3)_2$ and c) $0.5*10^{-3}$ M $Al(NO_3)_3$ at 30 °C and near CP.

Table 9: Micellar parameters of 0.03M TBADBS with varying salts at 30(^{o}C) and near CP.

0.03M TBADBS+Salt	Temperature (^{0}C)	Semi-minor axis b=c (Å)	Semi-major axis a (Å)	**Porod law (α)**	Remarks	Aggregation number N	Micellar fraction
No salt	30	18.5	200	-	-	366	1.0
	38	18.5	257	-	-	471	-
0.005MNaCl	30	16.0	91.4	-	-	125	1.0
	45	16.0	174.0	-	-	238	0.42
0.001Mg(NO$_3$)$_2$	30	17.0	101.4	-	-	157	1.0
	41	17.0	101.4	4	Porod scattering arising from large clouds	157	0.3
0.5*10^{-3} Al(NO$_3$)$_3$	30	16.8	97.6	-	-	147	1.0
	35	16.8	97.6	4	Porod scattering arising from large clouds	147	0.45

4.2.6. NMR measurements

The above salt induced structural changes were also monitored by collecting NMR data at different NaCl concentrations with 0.03M TBADBS (Figure 21). The spectra do not show any significant change in peak size/position indicating no considerable change in micellar morphology in this [NaCl] range at 30°C. The ^{1}H NMR spectra of 0.03M TBADBS in presence of 0.015M NaCl at different temperatures are shown in Figure 22. The data are quite interesting in the pre-clouding region (42-46°C). The disappearing/merging of peaks is a signal of grown micellar morphologies [183] which is in consonance to our proposition that higher order aggregates are present when the solution approaches the CP (as observed with DLS data). Similar morphological transitions with increasing temperature have been reported in the past with a mixed cationic-anionic surfactant system [112]. However, reappearance of peaks as well as their broadening indicates the presence of distinct morphologies of different sizes in the solution above the CP. The higher concentration studies with other inorganic salts ($Mg(NO_3)_2$ and $Al(NO_3)_3$) were hampered due to the appearance of clouding near the ambient temperature. Thus, from Figure 22, it can be said that temperature and salt has a synergistic effect on micellar growth. Thus it can be said that micellar growth and CP variation depend upon the hydrated radii of added counterion. The heat induced coexistence of micellar and / or vesicular region can also be acquired with simple salt like NaCl at moderate concentration in addition to the one having catanionic system [114].

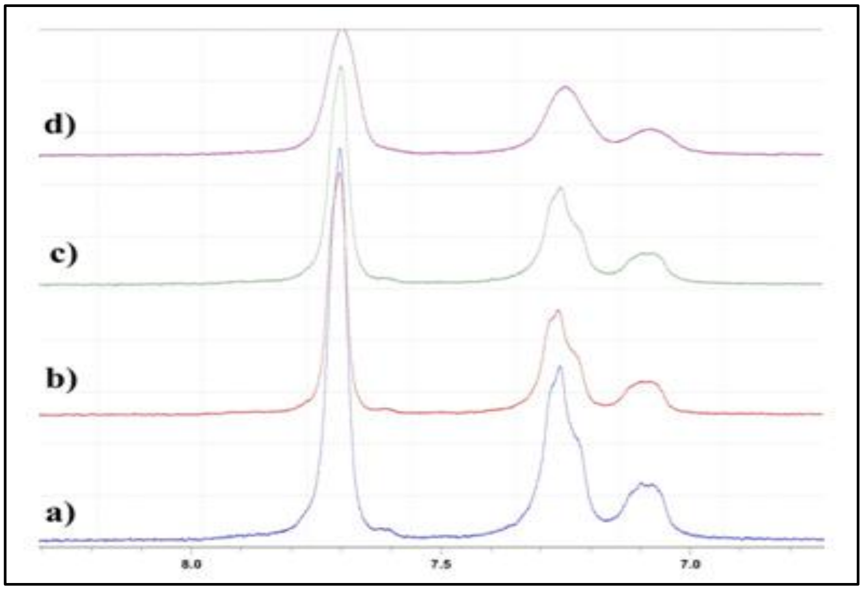

Figure 21: ^{1}H NMR spectra (400 MHz) for aromatic hydrocarbon protons in 0.03M TBADBS solution in presence of different concentrations of a) 0 M, b) 0.5 mM, c) 0.005 M and d) 0.015 M NaCl at 30 °C.

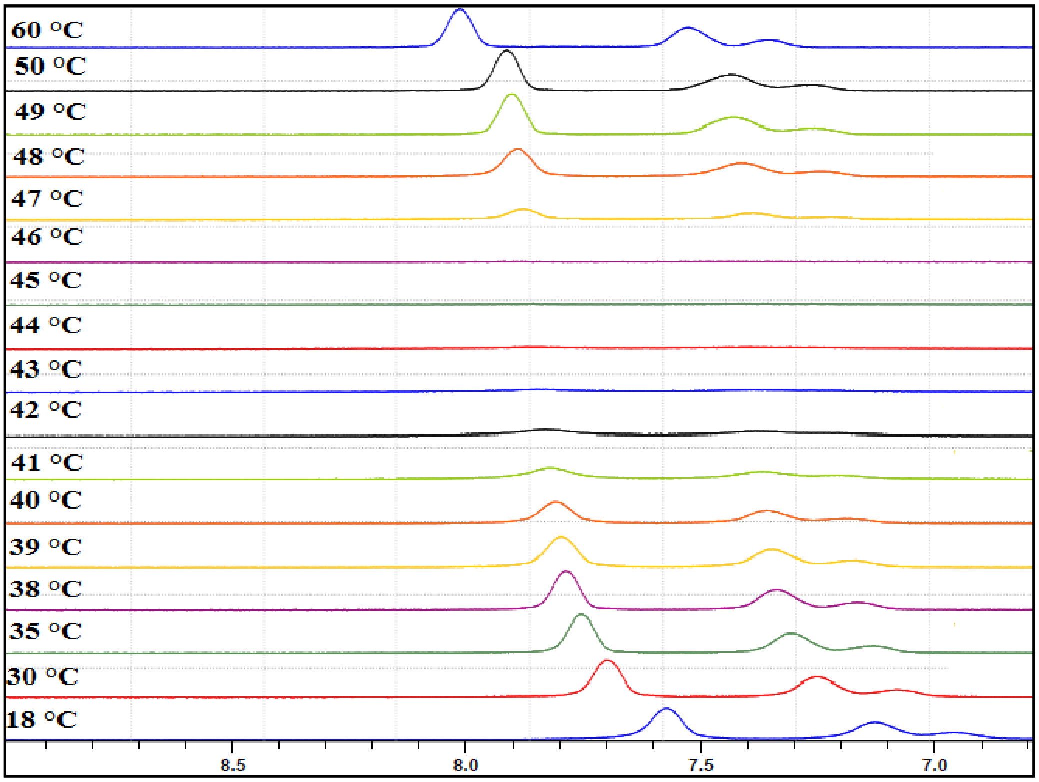

Figure 22: ^{1}H NMR spectra (400 MHz) for aromatic hydrocarbon protons in 0.03 M TBADBS solution in presence of 0.015 M NaCl at different temperatures.

4.2.7. Effect of conventional surfactants on clouding and the morphological transitions taking place near the CP.

SANS data at variable temperature could not be obtained with TBPDS and TBPDBS having TBP$^+$ counterion due to very dilute solutions (lower CPs at lower concentrations), lowering the scattering of neutrons. To get deeper insight into the mechanism of clouding the mixed micelle study is done using the quaternary and the conventional (SDS and TX-100) surfactants.

Generally when mixed micelle systems from nonionic and ionic are compared, the addition of SDS or CTAB increases the CP of known nonionic system. This may be due to the incorporated charge in the system. For the present quaternary surfactants too, the addition of above surfactants resulted in the increased CP. Surprisingly the decrease in overall charge along with the disintegration of micelles with increasing temperature is seen (Figure 23 and Table 10). Contrary to this, distinct micellar growth is seen in presence of TX-100 with the increasing temperature (Table 11). A typical SANS data with various [TX-100] are shown in Figure 24.

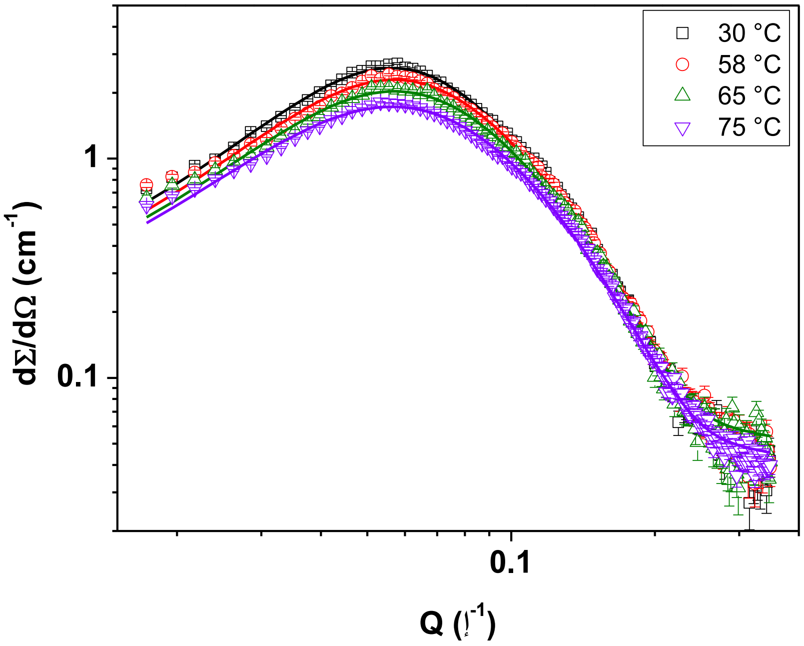

Figure 23: SANS spectra of 0.03M TBPDS+0.03MSDS below, at and above CP

Table 10: Micellar parameters of 0.03 M TBPDS in presence of 0.03M SDS at different temperatures using the prolate ellipsoidal model

Temperature (°C)	**Semi-major axis a (Å)**	**Semi-minor axis b=c (Å)**	**Charge Z (e.u.)**
30	38.9	15.0	21.3
58	**34.5**	**14.9**	**20.9**
65	32.6	15.2	20.3
75	31.9	15.0	18.8

Table 11: Compiled Micellar parameters of 0.03 M TBPDS with different [TX100] at different temperature using the oblate ellipsoidal model

Temperature (°C)	1%			2%			5%		
	Semi Major (b=c) (Å)	Semi Minor a (Å)	Charge Z (e.u.)	Semi Major (b=c) (Å)	Semi Minor a (Å))	Charge Z (e.u.)	Semi Major (b=c) (Å)	Semi Minor a (Å)	Charge Z (e.u.)
30	41.7	15.8	12.3	48.8	15.7	14.4	46.2	16.0	16.1
56	-	-		**65.2**	**16.0**	**8.8**	-	-	
58	**51.6**	**16.0**	**11.2**	-	-		-	-	
60				72.1	16.0	8.8	80.8	16.0	11.2
65	**52.0**	**16.0**	**1.8**	71.7	16.0	8.7	-	-	
75	**Porod scattering**			-	-	-	-	-	-

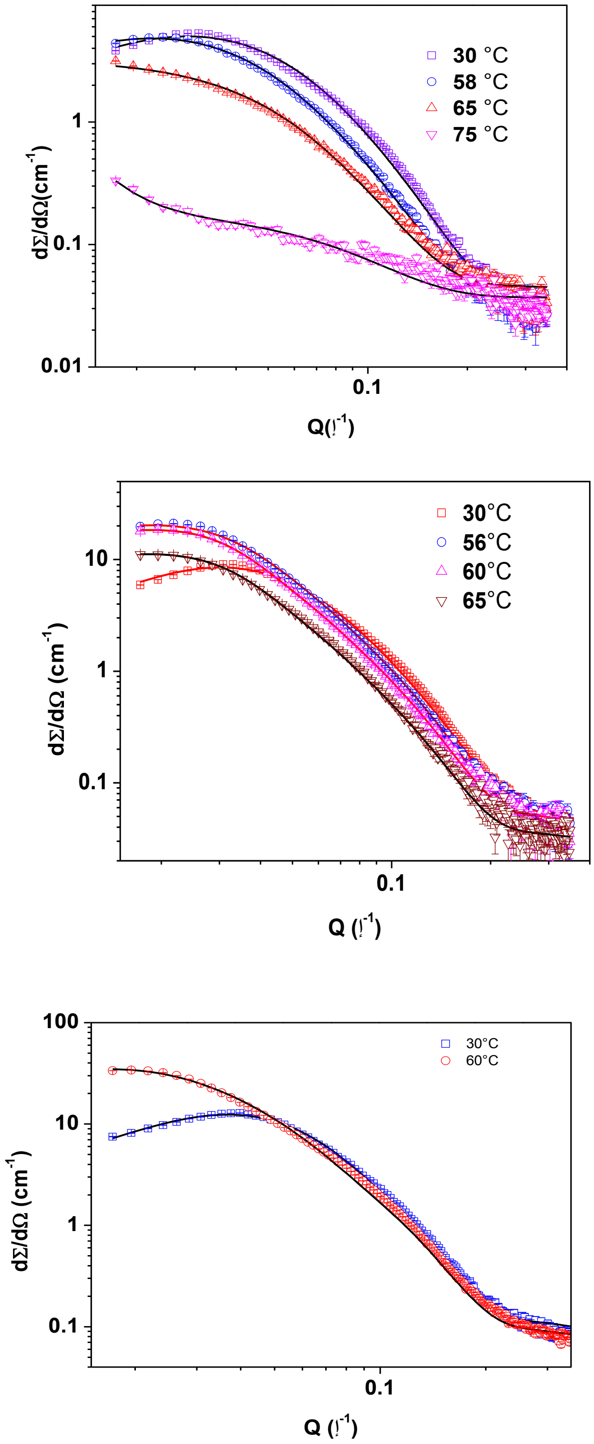

Figure 24: SANS spectra of 0.03M TBPDS+ a) 1%TX-100, b) 2%TX-100 and c) 5% TX100 at different temperatures

4.3 Conclusions

The study allows us to conclude that clouding phenomenon occurs gradually in quaternary surfactants when compared to that in nonionic surfactant solutions. This may be due to the presence of charged micelles in the former case. For clouding, only a small fraction of individual micelles is needed that convert into giant aggregates. Morphological changes, when the system approaches the CP, have been observed. NMR, SANS and DLS data depict the presence of two types of morphologies when the quaternary surfactant solutions as the temperature increases toward CP. The study shows unusual micellar growth on heating with the above surfactants, revealing an opposite trend to what it is reported for conventional anionic surfactant solution. The NMR results confirm the onset of attractive interactions among the grown micelles. Moreover, temperature and salt showed a synergistic effect with respect to micellar growth. Therefore, temperature can be used as an additional stimulus for micellar growth where presence of salt is undesirable. Also, the % of giant aggregates/micelle can be tuned by the [surfactant], temperature, [salt] and even by nature of salt. The effect of conventional surfactants on quaternary surfactants varies depending upon the charge. Addition of TX-100 results in micellar growth when the mixed system approaches CP. However, such micellar growth was weak on addition of anionic SDS.